Received: 21 November 2021 | Accepted: 9 March 2022

DOI: 10.1111/bpa.13069

RESEARCH ARTICLE

Brain Pathology

Independent distribution between tauopathy secondary to subacute sclerotic panencephalitis and measles virus: An immunohistochemical analysis in autopsy cases including cases treated with aggressive antiviral therapies

Hiroaki Miyahara[1,2] | Akio Akagi[2] | Yuichi Riku[2] | Jun Sone[2] | Yasushi Otsuka[3] | Motoko Sakai[4] | Satoshi Kuru[4] | Masato Hasegawa[5] | Mari Yoshida[2] | Akiyoshi Kakita[6] | Yasushi Iwasaki[2]

[1]Department of Pediatric Neuropathology, Institute for Medical Research of Aging, Aichi Medical University, Aichi, Japan

[2]Department of Neuropathology, Institute for Medical Research of Aging, Aichi Medical University, Aichi, Japan

[3]Department of Neurology, Toki General Hospital, Gifu, Japan

[4]Department of Neurology, National Hospital Organization Suzuka National Hospital, Mie, Japan

[5]Department of Brain and Neuroscience, Tokyo Metropolitan Institute of Medical Science, Tokyo, Japan

[6]Department of Pathology, Brain Research Institute, Niigata University, Niigata, Japan

Correspondence
Hiroaki Miyahara, Department of Neuropathology, Institute for Medical Science of Aging, Aichi Medical University, 1-1 Yazakokarimata, Nagakute, Aichi 480-1195, Japan.
Email: miyahara.hiroaki.926@mail.aichi-med-u.ac.jp

Funding information
AMED, Grant/Award Numbers JP18dm0107105, JP16kk0205009, and JP21wm0425019; Grants-in Aid from the Research Committee of CNS Degenerative Diseases, Research on Policy Planning and Evaluation for Rare and Intractable Diseases, Health, Labour and Welfare Sciences Research Grants, the Ministry of Health, Labour and Welfare, Japan

Abstract

Subacute sclerotic panencephalitis (SSPE) is a refractory neurological disorder after exposure to measles virus. Recently, SSPE cases have been treated with antiviral therapies, but data on the efficacy are inconclusive. Abnormal tau accumulation has been reported in the brain tissue of SSPE cases, but there are few reports in which this is amply discussed. Five autopsied cases diagnosed as definite SSPE were included in this study. The subject age or disease duration ranged from 7.6 to 40.9 years old or from 0.5 to 20.8 years, respectively. Cases 3 and 4 had been treated with antiviral therapies. All evaluated cases showed marked brain atrophy with cerebral ventricle dilatation; additionally, marked demyelination with fibrillary gliosis were observed in the cerebral white matter. The brainstem, cerebellum, and spinal cord were relatively preserved. Immunoreactivity (IR) against measles virus was seen in the brainstem tegmentum, neocortex, and/or limbic cortex of the untreated cases but was rarely seen in the two treated cases. Activated microglia were broadly observed from the cerebrum to the spinal cord and had no meaningful difference among cases. Neurofibrillary tangles characterized by a combination of 3- and 4-repeat tau were observed mainly in the oculomotor nuclei, locus coeruleus, and limbic cortex. IR against phosphorylated tau was seen mainly in the cingulate gyrus, oculomotor nuclei, and pontine tegmentum, and tended to be observed frequently in cases with long disease durations but also tended to decrease along with neuronal loss, as in Case 5, which had the longest disease duration. Since the distribution of phosphorylated tau was independent from that of measles virus, the tauopathy following SSPE was inferred to be the result of diffuse brain inflammation triggered by measles rather than a direct result of measles virus. Moreover, antiviral therapies seemed to suppress measles virus but not the progression of tauopathy.

KEYWORDS
autopsy, measles virus, neurofibrillary tangle, subacute sclerotic panencephalitis, tau

1 | BACKGROUND

Subacute sclerotic panencephalitis (SSPE), a slow viral infection induced by a mutated measles virus (known as an SSPE virus [1]), is a fatal neurological disorder marked by progressive psychomotor deficits and involuntary movement a few years or decades after exposure to measles virus [2]. Recently, SSPE cases have been treated with inosine pranobex (IP), interferon (IFN), or ribavirin (RBV) [3,4], but the data on the efficacy of these treatments are inconclusive.

Tauopathies are clinically, morphologically, and biochemically heterogeneous neurodegenerative diseases characterized by the deposition of abnormal tau protein in the central nervous system (CNS). Currently, tauopathies are classified into three groups, namely, 3-repeat (3R), 4-repeat (4R), and a combination of 3- and 4-repeat (3R + 4R) tauopathies, using tau western blotting and immunohistochemistry (IHC) [5]. Representative 3R tauopathies include Pick's disease and myotonic dystrophy; 4R tauopathies include progressive supranuclear palsy (PSP), corticobasal degeneration, argyrophilic grain disease, and globular glial tauopathy; and 3R + 4R tauopathies include Alzheimer's disease (AD), chronic traumatic encephalopathy (CTE), and primary age-related tauopathy (PART).

It was reported in approximately 2000 that abnormal tau protein was detected in the cerebrospinal fluid (CSF) [6] in SSPE; additionally, neurofibrillary tangles (NFTs), which are agglomerations of phosphorylated tau, were observed in the brain tissues of SSPE patients [7–10]. In some previous reports, SSPE viruses were revealed to be present in neurons and oligodendrocytes and hypothesized to be associated with the pathogenesis of tauopathy in SSPE [8,11], but there are few reports in which this is amply discussed, especially regarding tauopathies in treated SSPE cases. In this study, we investigated tauopathies in autopsied SSPE patients who had received aggressive antiviral therapies and compared them to those of patients who had not received such therapies.

2 | MATERIALS AND METHODS

2.1 | SSPE patients enrolled in this study

Five autopsied SSPE patients whose tissues were archived by the Aichi Medical University Karei Ikagaku Brain Resource Center and the Brain Research Institute of Niigata University between 1978 and 2019 were enrolled in this study. All patients were Japanese and had been diagnosed with definite SSPE based on the diagnostic criteria

TABLE 1 Clinical and autopsy information on subacute sclerotic panencephalitis cases

Case	1	2	3	4	5	Unit
Sex	F	M	M	M	F	
Pre-existing disease	−	−	−	−	−	
Age at measles exposure (A)	0.6	1.0	2.1	0.8	0.6	y.o.
Age at onset (B)	7.1	7.0	17.3	22.3	6.7	y.o.
Age at death (C)	7.6	11.9	30.0	40.9	27.5	y.o.
Latent period (B–A)	6.5	6.0	15.2	21.5	6.1	Years
Disease duration (C–B)	0.5	4.9	12.7	18.6	20.8	years
Duration from exposure (C–A)	7.0	10.9	27.9	40.1	26.9	Years
Measles vaccination	−	−	+	−	+	
Periodic synchronous discharge	+	+	+	+	+	
Measles antibody in CSF	+	+	+	+	+	
Age at initiation of antiviral treatments	−	−	17.4	22.3	−	y.o.
Duration of antiviral treatments	−	−	0.5	NA	−	Years
Inosine pranobex	−	−	PO	−	−	
Interferon	−	−	ICV	IV	−	
Ribavirin	−	−	ICV	ICV	−	
Other treatments	PSL	−	−	PSL	−	
Tracheostomy	−	−	+	+	+	
Artificial respiratory management	0.2	−	−	−	0.3	Years
Brain weight	980	770	720	735	NA	Grams
Neuronal loss	+	+	+	+	++	
Cells with inclusion bodies on HE staining	++	+	−	−	++	

Abbreviations: CSF, cerebrospinal fluid; F, female; ICV, intracerebroventricular administration; IgG, immunoglobin G; IV, intravenous administration; M, male; NA, not available; PO, peroral administration; PSL, prednisolone; y.o., year(s) old.

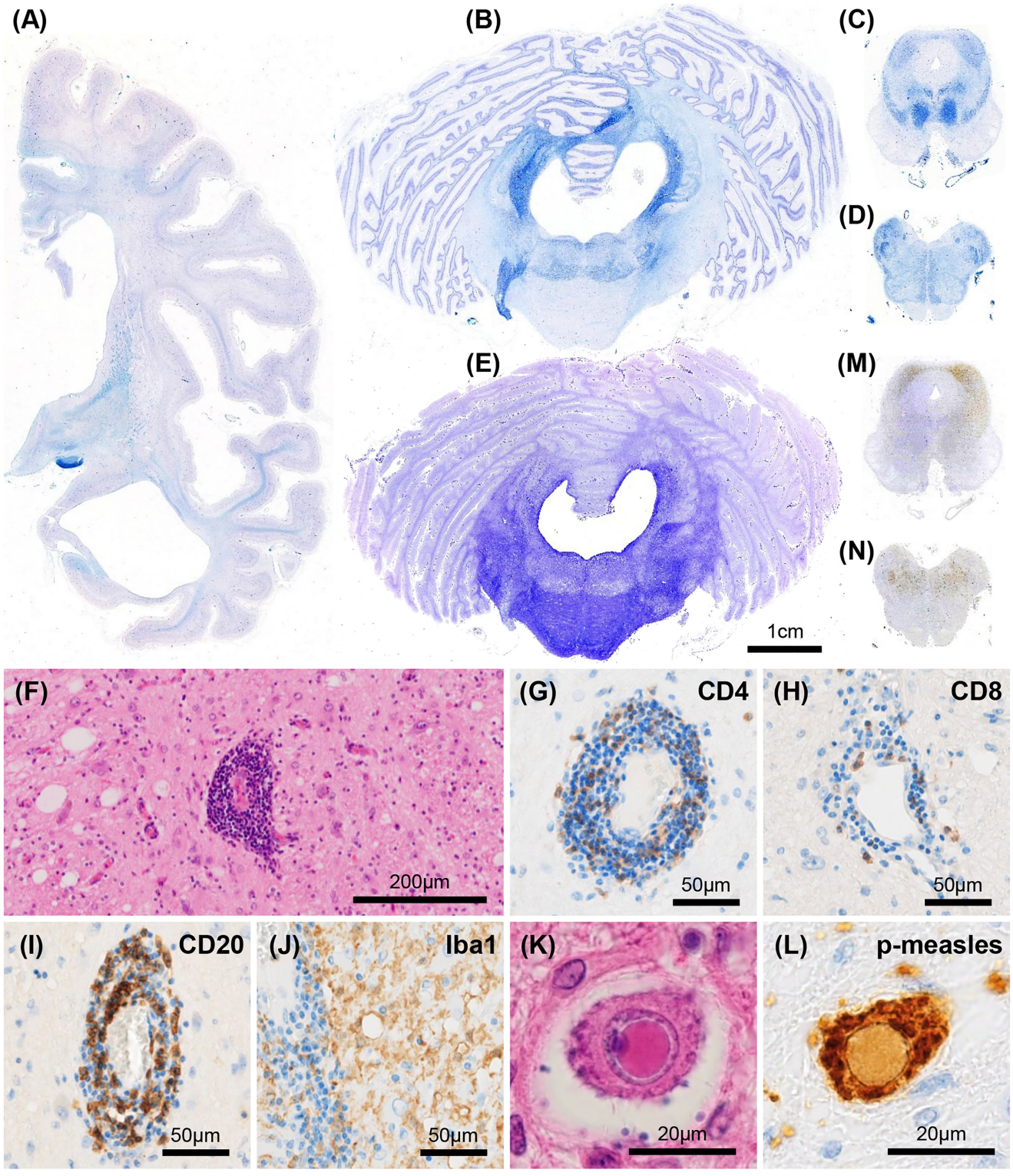

FIGURE 1 Common neuropathological findings in subacute sclerotic panencephalitis. (A–D) These images were taken from Case 2 and are representative of the five included cases. The cerebrums of these patients showed marked atrophy with cerebral ventricle dilatation, but the brainstems and cerebellums were relatively preserved. The myelin in the white matter (including the cerebrospinal tract) of these cases was poorly stained by Klüver–Barrera (KB) staining. (E) Gliotic scarring, which was visualized by Holzer staining, was observed mainly in the demyelinated white matter. (F) In active lesions, perivascular lymphocyte infiltrations and aggregations of hypertrophic astrocytes were noted. (G–J) The perivascular lymphocytes were composed chiefly of CD20+ or CD4+ lymphocytes. Abundant activated microglia were extensively observed in the active lesions. (K-N) Neurons with intranuclear inclusions, which were labeled using an antibody against measles virus, were frequently observed in the brainstem tegmentum. (A–D) KB staining; (E) Holzer staining; (F,K) hematoxylin and eosin staining; (G–J,M,N,L): immunohistochemistry for CD4 (G), CD8 (H), CD20 (I), Iba1 (J), and p-measles (M, N, L). Bar: 1 cm for (A–E,M,N), 200 μm for (F), 50 μm for (G–J), and 20 μm for (K,L)

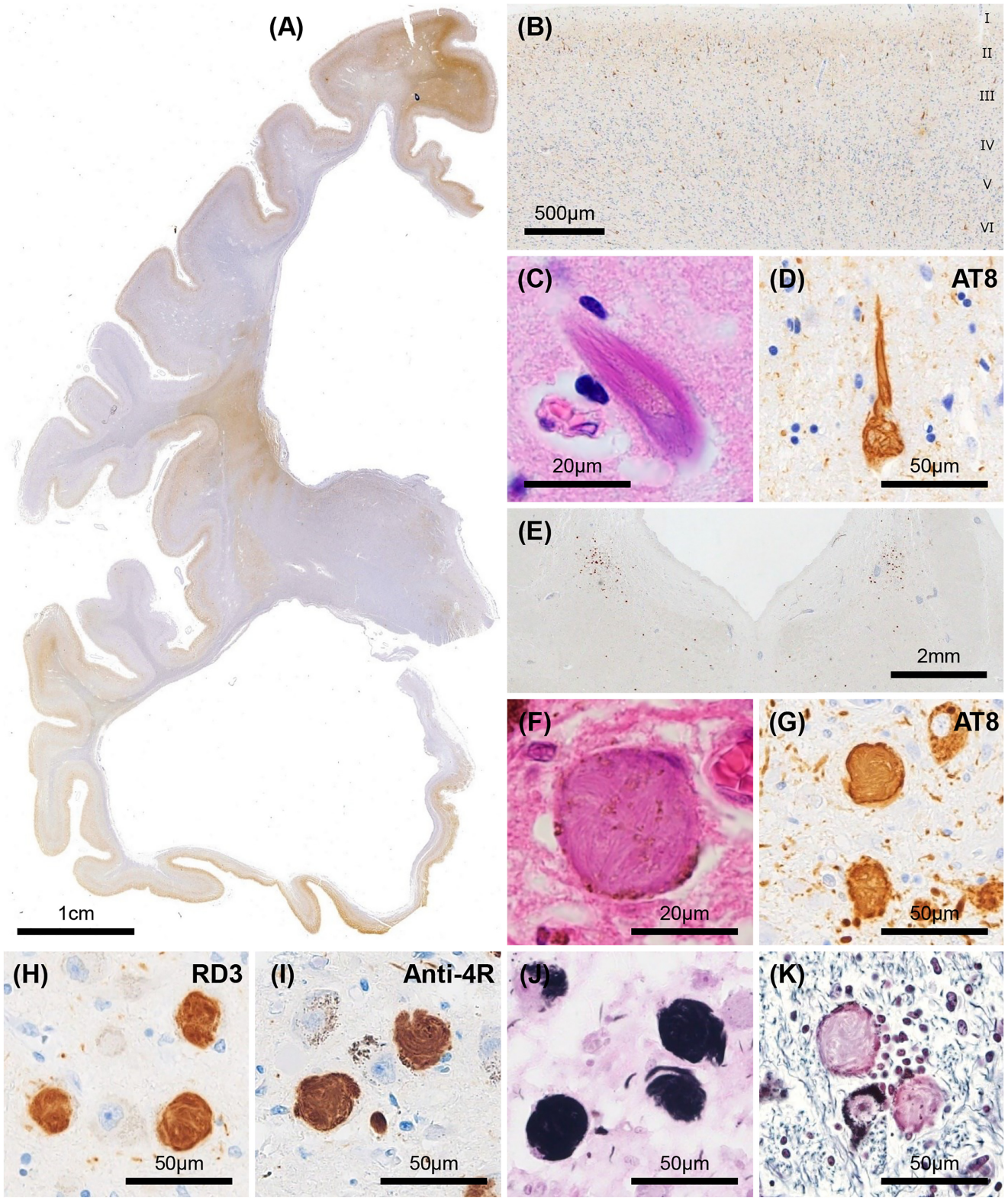

FIGURE 2 Representative pathology regarding tauopathy following subacute sclerotic panencephalitis. (A–K) These images were taken from Case 4. (A–C,E,F) Flame-shaped and globose-type neurofibrillary tangles (NFTs) were broadly distributed particularly in the superficial layers of the cerebral cortex, oculomotor nuclei, and locus coeruleus. (D,G–K) These NFTs were labeled by silver impregnation methods, such as Gallyas–Braak (J) and Bodian (K) staining, and immunostained with antibodies against AT8 (D,G), RD3 (H), and anti-4R (I). Bar: 1 cm for (A), 500 μm for (B), 20 μm for (C,F), 50 μm for (D,G–K), and 2 mm for (E)

proposed by Dyken [12] because they had a typical clinical course, periodic synchronous discharge (PSD) on electroencephalograms, and measles antibody positivity in CSF. The subject age or disease duration ranged from 7.6 to 40.9 years old or from 0.5 to 20.8 years, respectively. The immunoglobulin G index in CSF and the presence of a mutated measles virus genome were not evaluated. Two patients with pre-existing diseases, namely, acute lymphoblastic leukemia and suspected immunodeficiency, were excluded from this study. Cases 3 and 4 were treated by aggressive antiviral therapies including IP, IFN, and RBV (Table 1), but all patients had died within 21 years of onset.

2.2 | Histological and immunohistochemical analyses

Autopsied specimens were fixed with 20% buffered formalin and embedded in paraffin. Histological examinations were performed using sections processed by hematoxylin–eosin (HE), Klüver–Barrera (KB), Holzer, Gallyas-Braak, and Bodian staining. Immunohistochemical examinations were performed as previously described [13]. Briefly, the sections were incubated overnight with the following primary antibodies: anti-4R-tau antibody (polyclonal; CAC-TIP-4RT-P01; Cosmo Bio, Tokyo, Japan; 1:10,000, pretreated by heat antigen retrieval and formic acid), anti-α-synuclein antibody (polyclonal; S3062; Sigma-Aldrich, MO, USA; 1:20,000, pretreated by heat antigen retrieval and formic acid), anti-CD4 antibody (monoclonal; clone EPR6855; ab133616; Abcam, Cambridge, UK; 1:100, pretreated by heat antigen retrieval), anti-human CD8 antibody (monoclonal; clone C8/144B; M7103; DAKO, Glostrup, Denmark; 1:200, pretreated by heat antigen retrieval), anti-CD20 antibody (monoclonal; clone L26; NCL-L-CD20-L26; Leica Biosystems, Newcastle, UK; 1:200, pretreated by heat antigen retrieval), anti-human amyloidβ [1,3–5,8–11,13–22] antibody (monoclonal; clone 12B2; #10027; IBL, Spring Lake Park, MN, USA; 1:1000, pretreated by heat antigen retrieval and formic acid), anti-Iba1 antibody (polyclonal; #019-19741; FUJIFILM Wako Pure Chemical Corporation, Osaka, Japan; 1:2000, pretreated by heat antigen retrieval and formic acid), anti-p-measles virus antibody (monoclonal; clone 9H4; sc-101356; Santa Cruz Biotechnology, Santa Cruz, CA, USA; 1:100,000, pretreated by heat antigen retrieval), phospho-tau (Ser202, Thr205) antibody (monoclonal, clone AT8; MN1020; Thermo Scientific, Rockford, IL, USA; 1:5000), anti phospho TDP-43 (pS409/410) antibody (polyclonal; TIP-PTD-P07; CosmoBio, Tokyo, Japan; 1:4000; pretreated by heat antigen retrieval and formic acid), anti-tau (3R isoform RD3) antibody (monoclonal; clone 8E6/C11; #05-803; Upstate, Syracuse, NY, USA; 1:2500, pretreated by heat antigen retrieval and formic acid), and anti-tau (4R isoform RD4) antibody (monoclonal; clone 1E1/A6; #05-804; Millipore, Temecula, CA, USA; 1:500, pretreated by heat antigen retrieval and formic acid). Then, these sections were washed with phosphate-buffered saline five times for 5 min each and incubated with secondary antibody (Histofine Simple Stain MAX PO [MULTI]; Nichirei Bioscience Inc., Tokyo, Japan) for 1 h. The sections were visualized using 3,3′-diaminobenzidine (DAB; DAB Tablet; FUJIFILM, Osaka, Japan), and Mayer's hematoxylin solution was used as a counterstain. Neuronal loss was evaluated in the most affected regions of each case as – (none), + (1–50% loss), or ++ (>50% loss), and the abundance of cells with inclusion bodies on HE staining in the most readily visible regions of each case was evaluated as – (none), + [7,23–26],

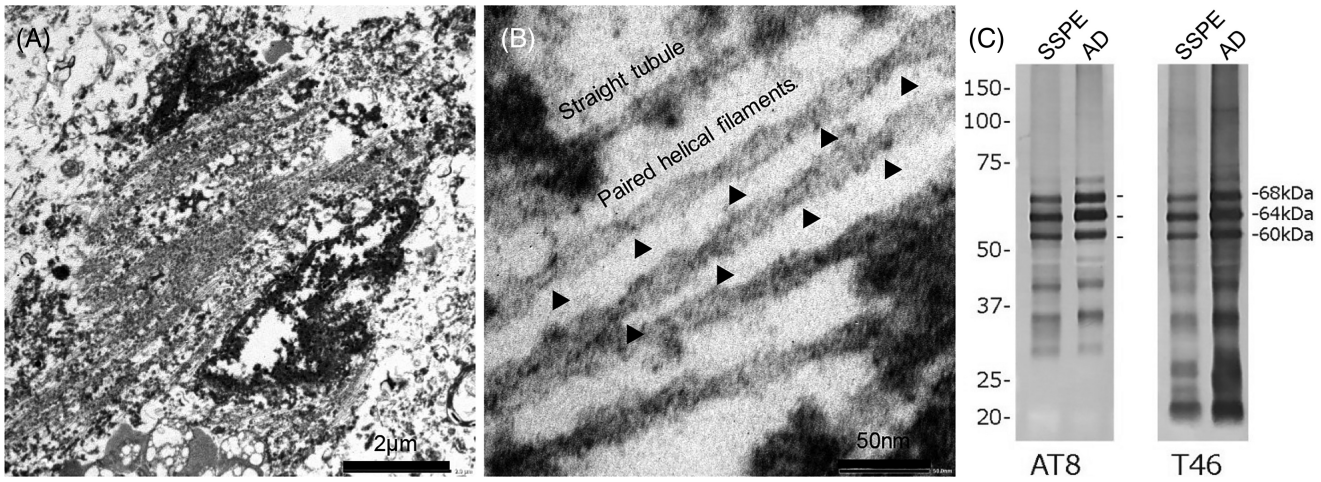

FIGURE 3 Electron microscopy and western blot in a case of tauopathy following subacute sclerotic panencephalitis. (A,B) By electron microscopy, the neurofibrillary tangles (NFTs) in the cingulate cortex of Case 4 were observed to be composed of paired helical filaments with a half-period of approximately 50 nm and straight tubules. (C) Western blots of the right cingulate cortex of Case 4 using AT8 and T46 antibodies showed triplet bands of 60, 64, and 68 kDa, the same molecular weights as the bands found in sample from Alzheimer's disease case. Bar: 2 μm for (A) and 50 nm for (B)

26], or ++ (>5) at ×40 objective magnification based on visual inspection.

2.3 | Semiquantitative measurement of the immunoreactivity in immunohistochemical analyses

Semiquantitative measurement of the immunoreactivity (IR) in the 25 anatomical regions shown in Figure 4 was performed to create distribution maps of measles virus, phosphorylated tau, and microglial infiltration. Immunohistochemical images using antibodies against p-measles virus (×40 objective magnification), AT8 (×20 objective magnification), and Iba1 (×20 objective magnification) were divided into DAB and hematoxylin images, and the mean gray value of the DAB images was semiquantitatively measured using the functions "Color deconvolution" and "Measure" in the software package ImageJ Ver. 1.440 (https://imagej.nih.gov/ij/). The mean gray values indicated ranged from 0 (black) to 255 (white) and were visualized as heatmaps using RStudio Desktop 1.1.463 (RStudio, Boston, MA, USA). The maximum mean gray value was set at 255, indicating no IR, and the minimum mean gray value was set at the value of the image showing the maximum IR in each IHC.

2.4 | Electron microscopic analysis of NFTs

Several pieces cut from a formalin-fixed cingulate cortex sample containing abundant NFTs in Case 4 were postfixed with 1% osmium tetroxide, dehydrated using a graded ethanol series, and embedded in Epon 812 (TAAB Epon 812, Nisshin-EM, Tokyo, Japan). Ultrathin sections were cut, stained with uranyl acetate and lead citrate, and examined with a JEM-1400 electron microscope (JEOL Ltd., Tokyo, Japan) at 80 kV.

2.5 | Western blotting of phosphorylated tau in a case with the tauopathy following SSPE

Tissue lysate obtained from the right cingulate cortex of the treated patient with a long disease duration (Case 4) was subjected to western blotting using anti-tau antibodies (AT8 and T46, Thermo Fisher, Waltham, MA, USA), as we described previously [19,23]. Brain lysate taken from a patient with AD (a male who died at 73 years of age) was also assessed for comparison.

3 | RESULTS

3.1 | Clinical and autopsy information in SSPE cases

As shown in Table 1, these patients were exposed to measles virus at 0.6–2.1 years of age, developed SSPE at 6.7–22.3 years of age, died at 7.6–40.9 years of age, and had a disease duration of 0.5–20.8 years. PSD and measles antibody in CSF were observed in all cases. In Cases 3 and 4, the patients underwent aggressive antiviral therapies using IP + IFN + RBV and IFN + RBV,

TABLE 2 Comparison between subacute sclerotic panencephalitis and other tauopathies forming neurofibrillary tangles

	SSPE	CTE	AD	PART	PSP
Tau isoform	3R + 4R	3R + 4R	3R + 4R	3R + 4R	4R
Primary affected regions of NFTs	Limbic BS	Neocortex	TEC	HC PHG	STh BG BS
NFT location in the cortical layer	II/III	II/III Perivascular Deep cerebral sulcus	III/V/VI	III–V	III–V
RD3 IHC	+	+	+	+	−
Anti-4R IHC	+	+	+	+	+
Silver impregnation	+	+	+	+	+
Characteristics of NFTs on EM	PHF/SF	PHF	PHF/SF	PHF	SF
WB using AT8 antibody (kDa)	60 64 68	60 64 68	60 64 68 (72)	60 64 68 (72)	60 64
References	[7,8,10] and our data	[5,27]	[5]	[5]	[5]

Abbreviations: AD, Alzheimer's disease; BG, basal ganglia; BS, brainstem; CTE, chronic traumatic encephalopathy; EM, electron microscopy; HC, hippocampus; IHC, immunohistochemistry; NFT, neurofibrillary tangle; PART, primary age-related tauopathy; PHF, paired helical filaments; PHG, parahippocampal gyrus; PSP, progressive supranuclear palsy; SF, straight filament; SSPE, subacute sclerotic panencephalitis; STh, subthalamic nucleus; TEC, transentorhinal cortex; WB, western blot.

respectively, within 3 months after the diagnosis. A tracheostomy was performed in Cases 3–5, and artificial respiratory management was performed in Cases 1 and 5.

3.2 | Common neuropathological findings in SSPE cases

The brain weights of all included patients were below the norm, ranging from 735 to 980 g. The patient's brain weight in Case 5 was not available, but the gross appearance of her brain indicated greater atrophy than any of the others. The cerebrums of these patients showed marked brain atrophy with cerebral ventricle dilatation, but their brainstems, cerebellums, and spinal cords were relatively preserved. The myelin of the white matter (including the corticospinal tract) in these cases was poorly stained by KB staining (Figure 1A–D), and gliotic scarring was observed mainly in the pale white matter by Holzer's staining (Figure 1E). Neuronal loss in the cerebral cortex, basal ganglia, thalamus, and hippocampus was seen in all cases but was accentuated in Case 5. The neuronal loss in the treated cases was mild for the long disease durations. In active lesions, perivascular lymphocyte infiltrations and aggregations of hypertrophic astrocytes were noted (Figure 1F). The perivascular lymphocytes were composed chiefly of CD20+ or CD4+ lymphocytes. Abundant activated microglia were extensively observed in the active lesions (Figure 1G–J). Neurons and glial cells with intranuclear inclusion bodies were observed using HE staining, but were visualized more frequently and broadly using an antibody against

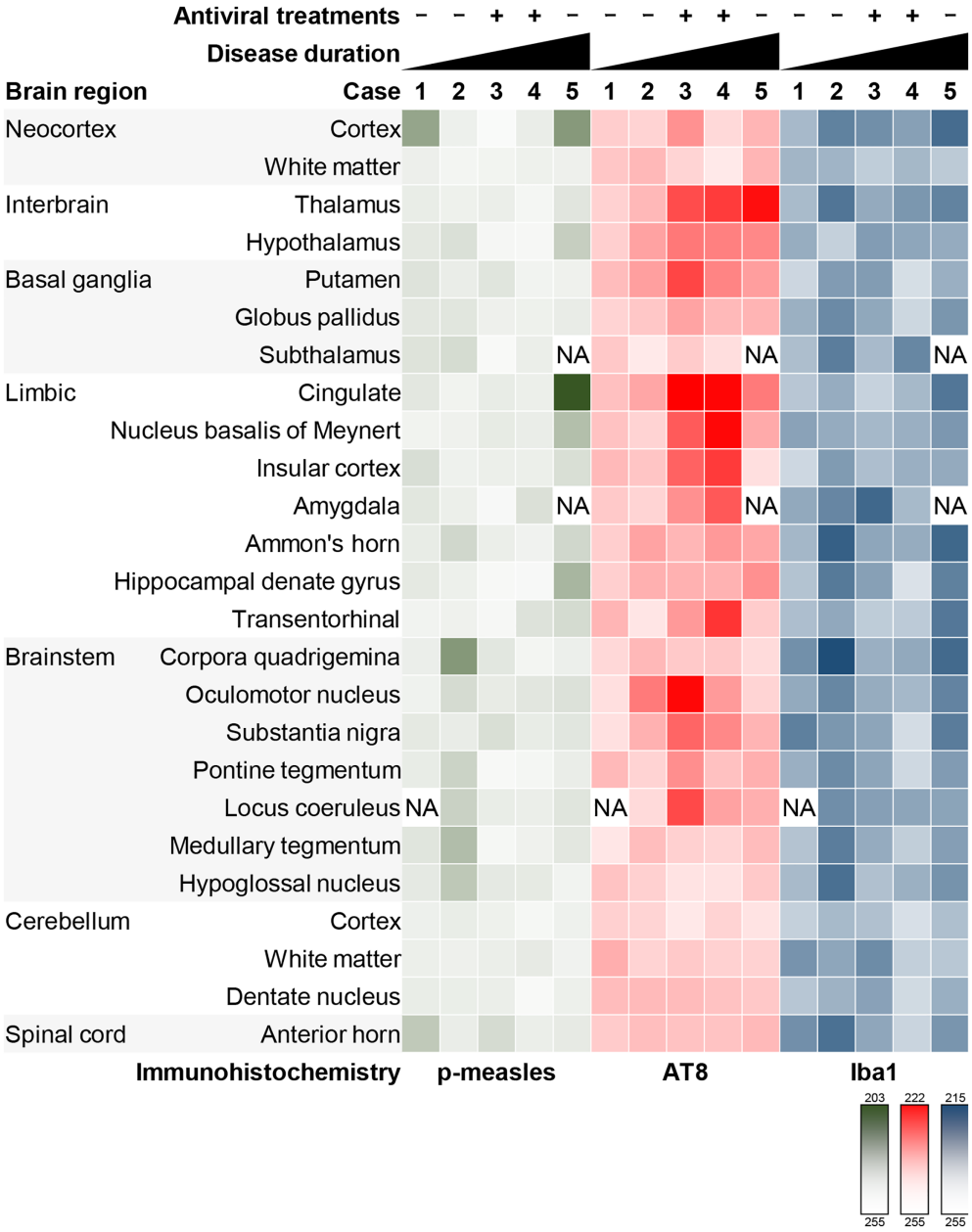

FIGURE 4 Heatmap visualization of the distributions of phosphorylated tau and measles virus in cases of subacute sclerotic panencephalitis. IR against measles virus was seen mainly in the tegmentum of the midbrain and pons, neocortex, and/or limbic cortex, and was rarely seen in the treated cases (Cases 2 and 3). IR against phosphorylated tau was seen mainly in the cingulate gyrus, the oculomotor nuclei, and/or the pontine tegmentum, and tended to be observed frequently in cases with long disease durations. Moreover, IR against Iba1 was broadly observed from the cerebrum to the spinal cord, and there was no meaningful difference in Iba1 expression among these cases. NA: not available

measles virus (Figure 1K,L). Abundant IR against measles virus was frequently observed in the brainstem tegmentum in Case 2 (Figure 1M,N) and in the neocortex and limbic regions in Cases 1 and 5. No amyloid plaques or cerebral amyloid angiopathy were visible upon amyloid-β immunostaining, and no abnormal inclusions labeled by antibodies against α-synuclein or phosphorylated TDP-43 were seen in these cases (data not shown).

3.3 | Representative tauopathy following SSPE

Flame-shaped NFTs were observed mainly in the superficial layers of the limbic cortex (Figure 2A–D), and globose-type NFTs were mainly observed in the oculomotor nuclei and locus coeruleus (Figure 2E–G). The NFTs were labeled by silver impregnation methods such as Bodian and Gallyas-Braak staining, and immunostained with antibodies against AT8, RD3, and anti-4R (Figure 2D,G–K) but not RD4 (data not shown). By electron microscopy, the NFTs were observed to be composed of paired helical filaments with a half-period of approximately 50 nm and straight tubules (Figure 3A,B). Western blots using AT8 and T46 antibodies showed triplet bands of 60, 64, and 68 kDa, the same molecular weights observed in sample from AD case (Figure 3C). The profiles of NFTs in silver impregnation, IHC, electron microscopy, and western blots were similar to those of AD [24]. Astrocytes with abnormal tau accumulation were seen in Case 5 but rarely in other cases.

3.4 | Heatmap visualization of the distribution of phosphorylated tau and measles virus in the SSPE cases

IR against measles virus was seen mainly in the brainstem tegmentum, neocortex, and/or limbic cortex and was rarely seen in the two treated cases. IR against phosphorylated tau was seen mainly in the cingulate gyrus, oculomotor nuclei, and pontine tegmentum and tended to be observed frequently in the cases with long disease durations, but this IR tended to decrease along with neuronal loss, as in Case 5, which had the longest disease duration. Moreover, IR against Iba1 was broadly observed from the cerebrum to the spinal cord, and there was no meaningful difference in Iba1 expression among these cases (Figure 4).

4 | DISCUSSION

In our study, NFTs were observed in the superficial layer of the limbic cortex, oculomotor nuclei, and locus coeruleus of SSPE cases with long disease durations, whereas measles virus was rarely seen in SSPE cases treated with aggressive antiviral therapies. Furthermore, NFTs following SSPE showed staining profiles consistent with those of 3R + 4R tauopathies, such as CTE, AD, and PART, but a notable difference between the NFTs of SSPE cases and those of other tauopathy cases was the occurrence of NFTs in the superficial layers of the limbic cortex.

As shown in Table 2, which presents a comparison between tauopathy following SSPE and other tauopathies forming NFTs (such as CTE, AD, PART, and PSP), tauopathy following SSPE was characterized by flame-shaped NFTs mainly in the superficial layer of the limbic cortex and globose-type NFTs in the brainstem tegmentum. These NFTs were consistent with the characteristics of 3R + 4R tauopathy. These characteristics of tauopathy following SSPE somewhat resemble those of CTE at the point of superficial occurrence, indicating that tauopathy following SSPE was the result of diffuse brain inflammation triggered by measles rather than the direct action of measles virus.

IP has a combination of effects, such as antiviral and immunostimulatory activity, and is reported to suppress symptom progression in 11%–66% of SSPE cases [12,14,15] 12,14,15] and to improve the 8-year survival rate from 8% to 61% [26]. IFN inhibits viral growth, and it was estimated to improve or arrest the progression of SSPE in 17%–50% or 22%–28% of cases, respectively [28,29]. RBV has a broad spectrum of activity against measles virus, and RBV was reported to improve clinical symptoms and reduce the titer of measles antibodies in CSF [17,20,21]. These reports, however, all focused on clinical symptoms and viral titers rather than pathological changes such as tauopathy. To our knowledge, there is no other report evaluating the efficacy of these antiviral therapies using the brains of autopsied SSPE patients.

A previous immunohistochemical investigation by McQuaid et al. regarding tauopathy in untreated SSPE cases indicated that numerous tau-positive NFTs were present in cases with a long disease duration (more than 2 years), and measles virus was detected in every case with a disease duration between 4 months and 18 years [10]. Their results regarding NFTs are compatible with ours, but the detection frequency of measles virus was apparently decreased in our treated cases. These results indicate that antiviral therapies might reduce the titer of SSPE virus in the CNS but are not able to suppress the progression of tauopathy following SSPE. Tau-targeting therapies such as tau hyperphosphorylation inhibitors [25,30], tau aggregation inhibitors [22], and immunotherapy against tau [16,18] are currently being investigated in clinical trials, and the combination of these tau-targeting and antiviral therapies might potently suppress tauopathy following SSPE.

Another immunohistochemical investigation by Bancher et al. regarding tauopathy in SSPE cases yielded a precise topographical analysis of phosphorylated tau and measles virus in an SSPE case with high numbers of both

NFTs and viral intranuclear inclusions [7]. Phosphorylated tau was distributed broadly throughout the patient's CNS but was less abundant in the medial temporal lobe, cerebellum, and medulla oblongata; these observations are fundamentally compatible with our results. Moreover, measles virus in his case was confined to the limbic system, including the medial temporal lobe. Regarding the distribution of measles virus in the CNS, there were too few evaluated cases to draw conclusions; more autopsied SSPE cases are needed to determine the localization of measles virus in the CNS.

Moreover, McQuaid et al. reported that an association between NFT formation and neuronal measles virus positivity was demonstrated in two cases with longer disease durations [10]; however, the distribution of phosphorylated tau and measles virus showed an independent association in our cases (Figure 4). Bancher et al. also proposed that NFT formation in SSPE was not restricted to locations containing measles virus antigen, which is compatible with our results [7]. Since the distribution of phosphorylated tau was independent from that of measles virus, tauopathy following SSPE was judged to be the result of diffuse brain inflammation triggered by measles infection rather than a direct result of measles virus.

The limitations of our study were a lack of direct confirmation of SSPE viral genome positivity and a small number of SSPE cases. SSPE viral genome positivity should be confirmed by PCR or in situ hybridization methods, but appropriate samples, such as wet samples and frozen tissue, were not available. Regarding the small number of SSPE cases, autopsied cases with SSPE have become extremely rare because of the widespread use of measles vaccinations in Japan.

5 | CONCLUSION

Tauopathy following SSPE was inferred to be the result of diffuse brain inflammation triggered by measles rather than a direct result of measles virus because the distribution of phosphorylated tau was independent from that of measles virus. Moreover, the current antiviral therapies for SSPE seemed to be effective for measles virus suppression but did not efficiently inhibit the progression of secondary tauopathy. The combination of antiviral and tau-targeting therapies is expected to induce favorable outcomes for SSPE cases in the future.

CONFLICT OF INTEREST

The authors declare no potential conflict of interest.

AUTHOR CONTRIBUTIONS

Hiroaki Miyahara conceptualized and designed the study. Mari Yoshida and Yasushi Iwasaki supervised the study. Jun Sone, Motoko Sakai, Satoshi Kuru, Yasushi Otsuka, and Akiyoshi Kakita contributed to the tasks of sample collection and data acquisition. Yuichi Riku and Akio Akagi assisted with the immunohistochemical and electron microscopic experiments, respectively. Masato Hasegawa conducted the western blot experiment. Hiroaki Miyahara performed the image analysis, visualized the data, and wrote the first draft of the manuscript. All authors contributed to the interpretation of the results, revised the first draft, and read and approved the final manuscript.

DATA AVAILABILITY STATEMENT

Data openly available in a public repository that issues datasets with DOIs

ETHICS STATEMENT

This study was performed in compliance with the principles of the Declaration of Helsinki. Approval was obtained from the institutional review boards of Aichi Medical University. Given the retrospective nature of the study, the requirement for informed consent was waived.

ORCID

Hiroaki Miyahara https://orcid.org/0000-0003-0723-0047

REFERENCES

1. Hotta H, Jiang DP, Nagano-Fujii M. SSPE virus and pathogenesis. Nihon Rinsho Jpn J Clin Med. 2007;65(8):1475–80.
2. Gutierrez J, Issacson RS, Koppel BS. Subacute sclerosing panencephalitis: an update. Dev Med Child Neurol. 2010;52(10):901–7.
3. Hashimoto K, Hosoya M. Advances in antiviral therapy for subacute sclerosing panencephalitis. Molecules. 2021;26(2):427.
4. Hosoya M. Anti SSPE drugs. Nihon Rinsho Jpn J Clin Med. 2012;70(4):625–8.
5. Kovacs GG. Invited review: neuropathology of tauopathies: principles and practice. Neuropathol Appl Neurobiol. 2015;41(1):3–23.
6. Yuksel D, Yilmaz D, Uyar NY, Senbil N, Gurer Y, Anlar B. Tau proteins in the cerebrospinal fluid of patients with subacute sclerosing panencephalitis. Brain Dev. 2010;32(6):467–71.
7. Bancher C, Leitner H, Jellinger K, Eder H, Setinek U, Fischer P, et al. On the relationship between measles virus and Alzheimer neurofibrillary tangles in subacute sclerosing panencephalitis. Neurobiol Aging. 1996;17(4):527–33.
8. Ikeda K, Akiyama H, Kondo H, Arai T, Arai N, Yagishita S. Numerous glial fibrillary tangles in oligodendroglia in cases of subacute sclerosing panencephalitis with neurofibrillary tangles. Neurosci Lett. 1995;194(1–2):133–5.
9. Maderna E, Fugnanesi V, Morbin M, Cacciatore F, Spinello S, Godani M, et al. Measles inclusion-body encephalitis: neuronal phosphorylated tau protein is present in the biopsy but not in the autoptic specimens of the same patient. Brain Pathol. 2016;26(4):542–6.
10. McQuaid S, Allen IV, McMahon J, Kirk J. Association of measles virus with neurofibrillary tangles in subacute sclerosing panencephalitis: a combined in situ hybridization and immunocytochemical investigation. Neuropathol Appl Neurobiol. 1994;20(2):103–10.
11. Isaacson SH, Asher DM, Godec MS, Gibbs CJ Jr, Gajdusek DC. Widespread, restricted low-level measles virus infection of brain in a case of subacute sclerosing panencephalitis. Acta Neuropathol. 1996;91(2):135–9.
12. Dyken PR. Subacute sclerosing panencephalitis. Current status. Neurol Clin. 1985;3(1):179–96.
13. Hirano M, Iritani S, Fujishiro H, Torii Y, Kawashima K, Sekiguchi H, et al. Globular glial tauopathy Type I presenting

with behavioral variant frontotemporal dementia. Neuropathology. 2020;40(5):515–25.
14. Haddad FS, Risk WS. Isoprinosine treatment in 18 patients with subacute sclerosing panencephalitis: a controlled study. Ann Neurol. 1980;7(2):185–8.
15. Huttenlocher PR, Mattson RH. Isoprinosine in subacute sclerosing panencephalitis. Neurology. 1979;29(6):763–71.
16. Lemere CA. Immunotherapy for Alzheimer's disease: hoops and hurdles. Mol Neurodegener. 2013;8:36.
17. Solomon T, Hart CA, Vinjamuri S, Beeching NJ, Malucci C, Humphrey P. Treatment of subacute sclerosing panencephalitis with interferon-alpha, ribavirin, and inosiplex. J Child Neurol. 2002;17(9):703–5.
18. Takeuchi H, Imamura K, Ji B, Tsukita K, Enami T, Takao K, et al. Nasal vaccine delivery attenuates brain pathology and cognitive impairment in tauopathy model mice. NPJ Vaccines. 2020;5:28.
19. Taniguchi-Watanabe S, Arai T, Kametani F, Nonaka T, Masuda-Suzukake M, Tarutani A, et al. Biochemical classification of tauopathies by immunoblot, protein sequence and mass spectrometric analyses of sarkosyl-insoluble and trypsin-resistant tau. Acta Neuropathol. 2016;131(2):267–80.
20. Tomoda A, Nomura K, Shiraishi S, Hamada A, Ohmura T, Hosoya M, et al. Trial of intraventricular ribavirin therapy for subacute sclerosing panencephalitis in Japan. Brain Dev. 2003;25(7):514–7.
21. Tomoda A, Nomura K, Shiraishi S, Miike T, Hamada A, Hosoya M. Trial of intraventricular ribavirin and interferon-alpha combination therapy for subacute sclerosing panencephalitis (SSPE) in Japan. No To Hattatsu. 2003;35(4):321–6.
22. Wischik CM, Staff RT, Wischik DJ, Bentham P, Murray AD, Storey JM, et al. Tau aggregation inhibitor therapy: an exploratory phase 2 study in mild or moderate Alzheimer's disease. J Alzheimers Dis. 2015;44(2):705–20.
23. Arai T, Ikeda K, Akiyama H, Nonaka T, Hasegawa M, Ishiguro K, et al. Identification of amino-terminally cleaved tau fragments that distinguish progressive supranuclear palsy from corticobasal degeneration. Ann Neurol. 2004;55(1):72–9.
24. Dan A, Takahashi M, Masuda-Suzukake M, Kametani F, Nonaka T, Kondo H, et al. Extensive deamidation at asparagine residue 279 accounts for weak immunoreactivity of tau with RD4 antibody in Alzheimer's disease brain. Acta Neuropathol Commun. 2013;1:54.
25. del Ser T, Steinwachs KC, Gertz HJ, Andrés MV, Gómez-Carrillo B, Medina M, et al. Treatment of Alzheimer's disease with the GSK-3 inhibitor tideglusib: a pilot study. J Alzheimers Dis. 2013;33(1):205–15.
26. DuRant RH, Dyken PR, Swift AV. The influence of inosiplex treatment on the neurological disability of patients with subacute sclerosing panencephalitis. J Pediatr. 1982;101(2):288–93.
27. Falcon B, Zivanov J, Zhang W, Murzin AG, Garringer HJ, Vidal R, et al. Novel tau filament fold in chronic traumatic encephalopathy encloses hydrophobic molecules. Nature. 2019;568(7752):420–3.
28. Gascon G, Yamani S, Crowell J, Stigsby B, Nester M, Kanaan I, et al. Combined oral isoprinosine-intraventricular alpha-interferon therapy for subacute sclerosing panencephalitis. Brain Dev. 1993;15(5):346–55.
29. Yalaz K, Anlar B, Oktem F, Aysun S, Ustacelebi S, Gurcay O, et al. Intraventricular interferon and oral inosiplex in the treatment of subacute sclerosing panencephalitis. Neurology. 1992;42(3 Pt 1):488–91.
30. Forlenza OV, Diniz BS, Radanovic M, Santos FS, Talib LL, Gattaz WF. Disease-modifying properties of long-term lithium treatment for amnestic mild cognitive impairment: randomised controlled trial. Br J Psychiatry. 2011;198(5):351–6.

How to cite this article: Miyahara H, Akagi A, Riku Y, Sone J, Otsuka Y, Sakai M, et al. Independent distribution between tauopathy secondary to subacute sclerotic panencephalitis and measles virus: An immunohistochemical analysis in autopsy cases including cases treated with aggressive antiviral therapies. Brain Pathology. 2022;32(6):e13069. https://doi.org/10.1111/bpa.13069